Hindawi Publishing Corporation
International Journal of Antennas and Propagation
Volume 2013, Article ID 169893, 7 pages
http://dx.doi.org/10.1155/2013/169893

Research Article

Analysis of High T_c Superconducting Rectangular Microstrip Patches over Ground Planes with Rectangular Apertures in Substrates Containing Anisotropic Materials

Abderraouf Messai,[1] Siham Benkouda,[1] Mounir Amir,[2] Sami Bedra,[2] and Tarek Fortaki[2]

[1] *Electronics Department, University of Constantine, 25000 Constantine, Algeria*
[2] *Electronics Department, University of Batna, 05000 Batna, Algeria*

Correspondence should be addressed to Tarek Fortaki; t_fortaki@yahoo.fr

Received 30 March 2013; Accepted 22 June 2013

Academic Editor: Haiwen Liu

A rigorous full-wave analysis of high T_c superconducting rectangular microstrip patch over ground plane with rectangular aperture in the case where the patch is printed on a uniaxially anisotropic substrate material is presented. The dyadic Green's functions of the considered structure are efficiently determined in the vector Fourier transform domain. The effect of the superconductivity of the patch is taken into account using the concept of the complex resistive boundary condition. The accuracy of the analysis is tested by comparing the computed results with measurements and previously published data for several anisotropic substrate materials. Numerical results showing variation of the resonant frequency and the quality factor of the superconducting antenna with regard to operating temperature are given. Finally, the effects of uniaxial anisotropy in the substrate on the resonant frequencies of different TM modes of the superconducting microstrip antenna with rectangular aperture in the ground plane are presented.

1. Introduction

Microstrip patch resonators offer many attractive features such as low profile, light weight, low cost, and the ease with which they can be integrated with printed feeding networks and active circuits. They can be used either as antennas or as components of oscillators and filters in microwave-integrated circuits. When a microstrip patch resonator acts as an antenna, the microstrip patch can be fed through an aperture cut into a microstrip line ground plane. Several advantages have been obtained by using this feeding configuration [1, 2]. Such advantages include weak parasitic radiation in the useful direction with respect to conventionally fed antennas and optimal performance for both the feeding network and antenna element. In addition, the presence of aperture on the ground plane adds new design parameters that can be used to tune the antenna impedance and resonance frequency, without modifying the patch itself. Since ground-plane apertures can play a role in the design of microstrip patch antennas, the algorithms developed for the analysis of these antennas should be able to account for the effect of possible apertures existing in the ground planes of the resonators.

Since the discovery of the high T_c superconducting materials which have critical temperatures above the boiling point of liquid nitrogen, the development of microwave application of high T_c superconductors has been extremely rapid and numbers of highly sophisticated subsystem level modules have been generated. Superconducting passive microwave devices such as antennas, filters, transmission line, and phase shifters have shown significant superiority over corresponding devices fabricated with normal conductors such as gold, silver, or copper due to the low surface resistance of superconductors. The low surface resistance corresponds to a large quality factor and improved performance such as higher gain and lower insertion loss in passive microwave devices [3–7].

Setting aside the topic of superconducting materials, in the last few years, there has been a growing interest in studying how the performance of microstrip antennas is

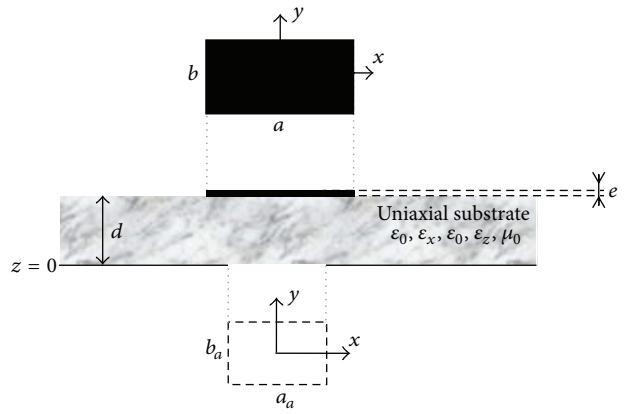

Figure 1: Geometrical structure of a high T_c superconducting rectangular microstrip patch over a ground plane with a rectangular aperture in the case where the superconducting patch is printed on an anisotropic dielectric substrate.

affected when anisotropic dielectrics are used as substrates of those antennas [8–14]. We bear in mind that some dielectric substances used as substrates of microstrip antennas exhibit anisotropy due to their natural crystal structures or as the result of their production processes. Isotropic substances may also exhibit anisotropy at high frequencies. The overall results of the previous studies indicate that operational behavior of such structures may not be as expected especially at higher millimetre wave frequencies when anisotropy of the substrate material is ignored.

This paper presents a rigorous full-wave analysis of high T_c superconducting rectangular microstrip patch over ground plane with rectangular aperture. The rectangular patch is printed on a uniaxially anisotropic substrate material. As far as the authors know, this subject has not been reported in the open literature; the only published results on the full-wave analysis of superconducting microstrip antennas with apertures in the ground planes refer to isotropic substrates [15]. This paper is organized as follows. In Section 2, the dyadic Green's functions of the considered structure are efficiently determined in the vector Fourier transform domain. The effect of the superconductivity of the patch is taken into account using the concept of the complex resistive boundary condition. Various numerical results are given in Section 3. Finally, concluding remarks are summarised in Section 4.

2. Theory

The problem to be solved is illustrated in Figure 1. We have a high T_c superconducting rectangular microstrip patch of thickness e over a ground plane with a rectangular aperture. The substrate material is uniaxially anisotropic with the optical axis being normal to the patch. The uniaxial substrate is characterized by the free-space permeability μ_0 and a permittivity tensor of the form

$$\bar{\boldsymbol{\varepsilon}} = \varepsilon_0 \begin{bmatrix} \varepsilon_x & 0 & 0 \\ 0 & \varepsilon_x & 0 \\ 0 & 0 & \varepsilon_z \end{bmatrix}, \tag{1}$$

where ε_0 is the free-space permittivity. Equation (1) can be specialized to the isotropic substrate by allowing $\varepsilon_x = \varepsilon_z = \varepsilon_r$. All fields and currents are time harmonic with the $e^{i\omega t}$ time dependence being suppressed. The transverse fields inside the anisotropic region ($0 < z < d$) can be obtained via the inverse vector Fourier transforms as shown in [16]

$$\begin{aligned} \mathbf{E}(\mathbf{r}_s, z) &= \begin{bmatrix} E_x(\mathbf{r}_s, z) \\ E_y(\mathbf{r}_s, z) \end{bmatrix} \\ &= \frac{1}{4\pi^2} \int\int_{-\infty}^{+\infty} \overline{\mathbf{F}}(\mathbf{k}_s, \mathbf{r}_s) \cdot \mathbf{e}(\mathbf{k}_s, z)\, dk_x dk_y, \\ \mathbf{H}(\mathbf{r}_s, z) &= \begin{bmatrix} H_y(\mathbf{r}_s, z) \\ -H_x(\mathbf{r}_s, z) \end{bmatrix} \\ &= \frac{1}{4\pi^2} \int\int_{-\infty}^{+\infty} \overline{\mathbf{F}}(\mathbf{k}_s, \mathbf{r}_s) \cdot \mathbf{h}(\mathbf{k}_s, z)\, dk_x dk_y, \end{aligned} \tag{2}$$

where $\overline{\mathbf{F}}(\mathbf{k}_s, \mathbf{r}_s)$ is the kernel of the vector Fourier transform [16], and

$$\begin{aligned} \mathbf{e}(\mathbf{k}_s, z) &= \begin{bmatrix} e^e(\mathbf{k}_s, z) \\ e^h(\mathbf{k}_s, z) \end{bmatrix} = \begin{bmatrix} \dfrac{i}{k_s} \dfrac{\varepsilon_z}{\varepsilon_x} \dfrac{\partial \widetilde{E}_z(\mathbf{k}_s, z)}{\partial z} \\ \dfrac{\omega\mu_0}{k_s} \widetilde{H}_z(\mathbf{k}_s, z) \end{bmatrix}, \\ \mathbf{h}(\mathbf{k}_s, z) &= \begin{bmatrix} h^e(\mathbf{k}_s, z) \\ h^h(\mathbf{k}_s, z) \end{bmatrix} = \begin{bmatrix} \dfrac{\omega\varepsilon_0\varepsilon_z}{k_s} \widetilde{E}_z(\mathbf{k}_s, z) \\ \dfrac{i}{k_s} \dfrac{\partial \widetilde{H}_z(\mathbf{k}_s, z)}{\partial z} \end{bmatrix}. \end{aligned} \tag{3}$$

The superscripts e and h denote the TM and TE waves, respectively, and $\widetilde{E}_z$ is the scalar Fourier transform of E_z. The general form of $\widetilde{E}_z$ and $\widetilde{H}_z$ is [17]

$$\begin{aligned} \widetilde{E}_z(\mathbf{k}_s, z) &= A^e e^{-ik_z^e z} + B^e e^{ik_z^e z}, \\ \widetilde{H}_z(\mathbf{k}_s, z) &= A^h e^{-ik_z^h z} + B^h e^{ik_z^h z}, \end{aligned} \tag{4}$$

where A^e, B^e, A^h, and B^h are the field spectral amplitudes and

$$\begin{aligned} k_z^e &= \left(\varepsilon_x k_0^2 - \frac{\varepsilon_x}{\varepsilon_z} k_s^2\right)^{1/2}, \qquad k_z^h = \left(\varepsilon_x k_0^2 - k_s^2\right)^{1/2}, \\ k_0^2 &= \omega^2 \varepsilon_0 \mu_0. \end{aligned} \tag{5}$$

k_z^e and k_z^h are, respectively, propagation constants for TM and TE waves in the uniaxially anisotropic substrate [2]. After

substitution of the expressions of $\widetilde{E}_z$ and $\widetilde{H}_z$ given by (4) into (3), we get [17]

$$\begin{aligned}\mathbf{e}(\mathbf{k}_s, z) &= \begin{bmatrix} e^e(\mathbf{k}_s, z) \\ e^h(\mathbf{k}_s, z) \end{bmatrix} \\ &= e^{-i\overline{\mathbf{k}}_z z} \cdot \mathbf{A}(\mathbf{k}_s) + e^{i\overline{\mathbf{k}}_z z} \cdot \mathbf{B}(\mathbf{k}_s), \\ \mathbf{h}(\mathbf{k}_s, z) &= \begin{bmatrix} h^e(\mathbf{k}_s, z) \\ h^h(\mathbf{k}_s, z) \end{bmatrix} \\ &= \overline{\mathbf{g}}(\mathbf{k}_s) \cdot \left[e^{-i\overline{\mathbf{k}}_z z} \cdot \mathbf{A}(\mathbf{k}_s) - e^{i\overline{\mathbf{k}}_z z} \cdot \mathbf{B}(\mathbf{k}_s) \right]. \end{aligned} \tag{6}$$

In (6), **A**, and **B** are two-component unknown vectors and

$$\overline{\mathbf{k}}_z = \begin{bmatrix} k_z^e & 0 \\ 0 & k_z^h \end{bmatrix}, \qquad \overline{\mathbf{g}}(\mathbf{k}_s) = \begin{bmatrix} \dfrac{\omega\varepsilon_0\varepsilon_x}{k_z^e} & 0 \\ 0 & \dfrac{k_z^h}{\omega\mu_0} \end{bmatrix}. \tag{7}$$

Writing (6) in the planes $z = 0$ and $z = d$, and by eliminating the unknowns **A** and **B**, we obtain the matrix form

$$\begin{bmatrix} \mathbf{e}(\mathbf{k}_s, d^-) \\ \mathbf{h}(\mathbf{k}_s, d^-) \end{bmatrix} = \overline{\mathbf{T}} \cdot \begin{bmatrix} \mathbf{e}(\mathbf{k}_s, 0^+) \\ \mathbf{h}(\mathbf{k}_s, 0^+) \end{bmatrix} \tag{8}$$

with

$$\overline{\mathbf{T}} = \begin{bmatrix} \overline{\mathbf{T}}^{11} & \overline{\mathbf{T}}^{12} \\ \overline{\mathbf{T}}^{21} & \overline{\mathbf{T}}^{22} \end{bmatrix} = \begin{bmatrix} \cos(\overline{\mathbf{k}}_z d) & -i\overline{\mathbf{g}}^{-1} \cdot \sin(\overline{\mathbf{k}}_z d) \\ -i\overline{\mathbf{g}} \cdot \sin(\overline{\mathbf{k}}_z d) & \cos(\overline{\mathbf{k}}_z d) \end{bmatrix}, \tag{9}$$

which combines **e** and **h** on both sides of the anisotropic region as input and output quantities. Now that we have the matrix representation of the anisotropic substrate, it is easy to derive the dyadic Green's functions of the problem. Let $\mathbf{J}_0(x, y)$ be the surface current density on the ground plane with rectangular aperture, and let $\mathbf{J}(x, y)$ be the surface current density on the superconducting rectangular patch. Also, let $\mathbf{E}(x, y, 0)$ and $\mathbf{E}(x, y, d)$ be the values of the transverse electric field at the plane of the aperture and at the plane of the superconducting patch, respectively. Following a mathematical reasoning similar to that shown in [16], we can obtain a relation among $\mathbf{J}_0(x, y)$, $\mathbf{J}(x, y)$, $\mathbf{E}(x, y, 0)$, and $\mathbf{E}(x, y, d)$ in the vector Fourier transform domain given by

$$\mathbf{e}(\mathbf{k}_s, d) = \overline{\mathbf{G}}(\mathbf{k}_s) \cdot \mathbf{j}(\mathbf{k}_s) + \overline{\mathbf{\Gamma}}(\mathbf{k}_s) \cdot \mathbf{e}(\mathbf{k}_s, 0), \tag{10}$$

$$\mathbf{j}_0(\mathbf{k}_s) = -\overline{\mathbf{\Gamma}}(\mathbf{k}_s) \cdot \mathbf{j}(\mathbf{k}_s) + \overline{\mathbf{Y}}(\mathbf{k}_s) \cdot \mathbf{e}(\mathbf{k}_s, 0), \tag{11}$$

where the 2×2 diagonal matrices $\overline{\mathbf{G}}(\mathbf{k}_s)$, $\overline{\mathbf{\Gamma}}(\mathbf{k}_s)$, and $\overline{\mathbf{Y}}(\mathbf{k}_s)$ stand for a set of dyadic Green's functions in the vector Fourier transform domain. It is to be noted that $\overline{\mathbf{G}}(\mathbf{k}_s)$ is related to the patch current and $\overline{\mathbf{Y}}(\mathbf{k}_s)$ is related to the aperture field. The matrix $\overline{\mathbf{\Gamma}}(\mathbf{k}_s)$ represents the mutual coupling between the patch current and aperture field. Considering the superconducting effect, we need simply to modify (10) by replacing $\overline{\mathbf{G}}(\mathbf{k}_s)$ by $\overline{\mathbf{G}}_s(\mathbf{k}_s) = \overline{\mathbf{G}}(\mathbf{k}_s) - Z_s \cdot \overline{\mathbf{I}}$, where $\overline{\mathbf{I}}$ stands for the 2×2 unit matrix and Z_s is the surface impedance of the superconducting patch. When the thickness of the superconducting patch is less than three times the zero-temperature penetration depth (λ_0), Z_s can be expressed as follows [7, 15]:

$$Z_s = \frac{1}{e\sigma}, \tag{12}$$

where σ is the complex conductivity of the superconducting film. It is determined by using London's equation and the Gorter-Casimir two-fluid model as [7, 15]

$$\sigma = \sigma_n \left(\frac{T}{T_c} \right)^4 - i \frac{1 - (T/T_c)^4}{\omega\mu_0\lambda_0^2}, \tag{13}$$

where T is the temperature, T_c is the transition temperature, σ_n is the normal state conductivity at $T = T_c$, and ω is the angular frequency. Now that we have included the effect of the superconductivity of the rectangular patch in the Green's functions formulation, the well-known Galerkin procedure of the moment method can be easily applied to obtain the resonant frequencies and quality factors of the resonant modes of the high T_c superconducting rectangular microstrip patch shown in Figure 1.

Using the moment method, with weighting modes chosen to be identical to the expansion modes, (10) and (11) are reduced to a system of linear equations which can be written compactly in matrix form as [17]

$$\overline{\mathbf{Z}} \cdot \mathbf{C} = \mathbf{0}, \tag{14}$$

where $\overline{\mathbf{Z}}$ is the impedance matrix and the elements of the vector **C** are the modes expansion coefficient to be sought [17]. The system of linear equations given in (14) has nontrivial solutions when

$$\det\left[\overline{\mathbf{Z}}(\omega)\right] = 0. \tag{15}$$

Equation (15) is an eigenequation for ω, from which the resonant frequency and quality factor of the structure of Figure 1 can be obtained. In fact, let $\omega = 2\pi(f_r + if_i)$ be the complex root of (15). In that case, the quantity f_r stands for the resonant frequency and the quantity $Q = f_r/(2f_i)$ stands for the quality factor.

3. Numerical Results and Discussion

3.1. Comparison of Numerical Results. In this study, the considered mode is the TM_{01} mode with the dominant current in the y direction (higher order TM modes are considered only in Section 3.4). The basis functions considered here for approximating the unknown current on the superconducting rectangular patch are formed by the set of TM modes of a rectangular cavity with magnetic side walls and electric top and bottom walls. Also, the same basis functions are used for approximating the magnetic current density on the aperture in accordance with the concept of complementary electromagnetic structures [1, 2].

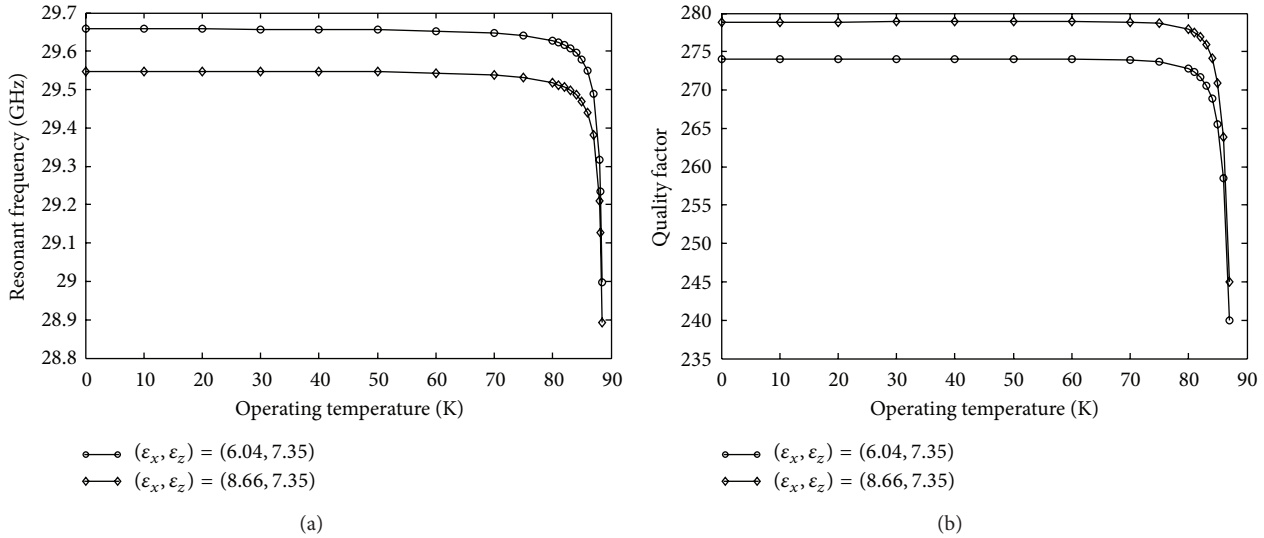

Figure 2: Resonant frequency and quality factor of the high T_c superconducting rectangular microstrip patch over ground plane with rectangular aperture against operating temperature. The superconducting patch is printed on two different anisotropic substrate materials; $a \times b = 1630\,\mu\text{m} \times 1870\,\mu\text{m}$, $a_a \times b_a = 53\,\mu\text{m} \times 187\,\mu\text{m}$, $d = 56.1\,\mu\text{m}$, $\sigma_n = 10^6$ S/m, $\lambda_0 = 140$ nm, $T_c = 89$ K, and $e = 350$ nm.

To check the correctness of our computer program, our numerical results are compared with those obtained from the magnetic-wall cavity model of Richard et al. [18], when there is no aperture in the ground plane. Numerical evaluations have been done with a patch of dimension 1.5 cm × 1 cm printed on anisotropic substrates. The patch is fabricated with a YBCO superconducting thin film with parameters $\sigma_n = 10^6$ S/m, $\lambda_0 = 140$ nm, $T_c = 89$ K, and $e = 350$ nm. The operating temperature is $T = 60$ K. Table 1 summarizes our computed resonant frequencies and those obtained via the magnetic-wall cavity model [18] for four different nonmagnetic anisotropic substrate materials. These anisotropic materials are Sapphire, Epsilam-10, Pyrolytic boron nitride, and PTFE. It is clear from Table 1 that the agreement between our results and those obtained via the magnetic-wall cavity model [18] is very good since the discrepancies between the two sets of results are below 1%. Note that in order to make the magnetic-wall cavity model of Richard et al. [18] able to account for uniaxial anisotropy in the substrate, we have associated with this model the electromagnetic knowledge [13]. The idea is to determine effective parameters for the uniaxially anisotropic substrate using [13, Equations (3) and (4)], and then we use these parameters in the magnetic-wall cavity model of Richard et al. [18].

We have also compared our results with experimental data available in the literature [18]. Table 2 shows the comparison between our calculations and the theoretical and experimental results reported in [18]. It is clear from Table 2 that our results are better than the theoretical values in [18]. The previous comparisons show a very good agreement between our results and those of the literature. This validates the theory proposed in this paper.

3.2. Influence of the Temperature on the Resonant Frequency and Quality Factor. Now, we investigate the influence of the operating temperature on the resonant frequency and quality factor of the superconducting rectangular microstrip antenna with a rectangular aperture in the ground plane. The patch of size $1630\,\mu\text{m} \times 1870\,\mu\text{m}$ is made of 350 nm thick YBCO thin film with a normal state conductivity at the transition temperature $\sigma_n = 10^6$ S/m, a zero-temperature penetration depth $\lambda_0 = 140$ nm, and a transition temperature $T_c = 89$ K. The rectangular aperture has a size of $53\,\mu\text{m} \times 187\,\mu\text{m}$. The resonant frequency and the quality factor of the superconducting antenna against operating temperature for two different anisotropic substrate materials are shown in Figures 2(a) and 2(b), respectively. The first uniaxially anisotropic material has the pair of relative permittivities $(\varepsilon_x, \varepsilon_z) = (6.04, 7.35)$. The second uniaxially anisotropic material is characterized by an electric anisotropy of negative type [14] ($(\varepsilon_x, \varepsilon_z) = (8.66, 7.35)$). Each dielectric substrate has a thickness of $56.1\,\mu\text{m}$. From the results of Figure 2(a) (Figure 2(b)), it is found that the resonant frequencies (quality factors) obtained when the superconducting patch is printed on the first anisotropic material are higher (lower) than those obtained when the superconducting patch is printed on the second anisotropic material because the effective relative permittivity of the first uniaxial medium is lower than the one of second uniaxial medium. Concerning the influence of the operating temperature on the resonant frequency and quality factor of the superconducting microstrip patch shown in Figure 1, it can be seen that the effect of varying the temperature on the resonant frequency and quality factor is significant only for temperatures near the transition temperature. Note that the steep change in the resonant frequency and quality factor at temperatures near T_c can be attributed to a change in the magnetic penetration depth of the YBCO [18].

3.3. Influence of Uniaxial Anisotropy in the Substrate on the Resonant Frequency. In Table 3, results are presented for the

Table 1: Comparison of our calculated resonant frequencies with those obtained via the cavity model [18] combined with electromagnetic knowledge [13] for various anisotropic substrate materials; $a \times b = 1.5\,\text{cm} \times 1\,\text{cm}$, $a_a = 0$, $d = 0.2\,\text{mm}$, $\sigma_n = 10^6\,\text{S/m}$, $\lambda_0 = 140\,\text{nm}$, $T_c = 89\,\text{K}$, $e = 350\,\text{nm}$, and $T = 60\,\text{K}$.

Anisotropic substrate		Resonant frequency (GHz)		
Dielectric	$(\varepsilon_x, \varepsilon_z)$	This work	Cavity model [18] combined with electromagnetic knowledge [13]	Error (%)
Sapphire	(9.4, 11.6)	4.371	4.363	0.18
Epsilam-10	(13, 10.3)	4.631	4.620	0.24
Pyrolytic boron nitride	(5.12, 3.4)	7.996	8.034	0.47
PTFE	(2.88, 2.43)	9.428	9.515	0.92

Table 2: Comparison of our calculated resonant frequencies with the theoretical and experimental data reported in [18]; $a \times b = 1630\,\mu\text{m} \times 935\,\mu\text{m}$, $\varepsilon_r = 23.81$, $d = 254\,\mu\text{m}$, $a_a = 0$, $\sigma_n = 10^6\,\text{S/m}$, $\lambda_0 = 140\,\text{nm}$, $T_c = 89\,\text{K}$, and $e = 350\,\text{nm}$.

Temperature (K)	Resonant frequencies (GHz)		
	Our results	Theoretical data [18]	Experimental data [18]
50	28.764	28.906	28.660
87.4	28.634	28.744	28.380

resonant frequencies of rectangular microstrip patch over ground planes with and without rectangular apertures in the case where the high T_c superconducting patch is printed on an anisotropic dielectric substrate, that is, Pyrolytic boron nitride, which exhibits a negative uniaxial anisotropy. The patch of size $1.5\,\text{cm} \times 1\,\text{cm}$ is fabricated with a YBCO superconducting thin film with parameters $\sigma_n = 10^6\,\text{S/m}$, $\lambda_0 = 140\,\text{nm}$, $T_c = 89\,\text{K}$, and $e = 350\,\text{nm}$. The substrate has a thickness of 1 mm. The operating temperature is $T = 50\,\text{K}$. In Table 3, the results obtained for the high T_c superconducting patch printed on anisotropic Pyrolytic boron nitride are compared with the results that would be obtained if the anisotropy of Pyrolytic boron nitride were neglected. In the case where $a_a \times b_a = a \times b$, the differences between the results obtained considering anisotropy and neglecting anisotropy are 5.45%. However, in the other considered cases, these differences are much smaller with the maximum change being 2.70% when $a_a \times b_a = 0.75a \times 0.75b$. Therefore, dielectric anisotropy effect is especially significant when the size of the aperture is similar to that of the high T_c superconducting patch. This result agrees with that discovered theoretically for perfectly conducting rectangular microstrip patches over ground planes with rectangular apertures [2].

3.4. Effect of the Anisotropy on Different Modes of the Superconducting Antenna. In Table 4, the effect of uniaxial anisotropy in the substrate on the resonant frequencies of superconducting rectangular microstrip patch over ground plane with rectangular aperture is also investigated. In this table, the considered dielectric is Sapphire, which exhibits a positive uniaxial anisotropy. Unlike Section 3.3, both fundamental mode and higher order TM modes are considered. The patch of size $1.5\,\text{cm} \times 1\,\text{cm}$ is fabricated with a YBCO superconducting thin film with parameters $\sigma_n = 10^6\,\text{S/m}$, $\lambda_0 = 140\,\text{nm}$, $T_c = 89\,\text{K}$, and $e = 350\,\text{nm}$. The substrate has a thickness of 2 mm, and the aperture size is $2.1\,\text{mm} \times 1.4\,\text{mm}$. The operating temperature is $T = 40\,\text{K}$. For the modes having the dominant current in the x direction (TM_{10} and TM_{20}), the differences between the results obtained considering anisotropy and neglecting anisotropy are smaller compared to those of the other considered modes. It is also seen from Table 4 that for the mode TM_{02}, the difference between the results obtained considering anisotropy and neglecting anisotropy is 2.27%. However, in the other considered modes, these differences are much smaller with the maximum change being 1.72% for the mode TM_{11}. Therefore, dielectric anisotropy effect is especially significant for the mode TM_{02}.

4. Conclusion

We have described an accurate analysis of high T_c superconducting rectangular microstrip patch over ground plane with rectangular aperture in the case where the superconducting patch is printed on an anisotropic dielectric substrate. The dyadic Green's functions of the considered anisotropic structure have been efficiently determined in the vector Fourier transform domain. The effect of the superconductivity of the patch has been taken into account using the concept of the complex resistive boundary condition. Galerkin's method has been used to solve for the surface current density on the superconducting patch and the transverse electric field at the aperture. The accuracy of the method was checked by performing a set of results in terms of resonant frequencies for various anisotropic substrate materials. In all cases, very good agreements compared with the literature were obtained. Numerical results show that the influence of the operating temperature on the resonant frequency and quality factor of superconducting rectangular microstrip patches over ground planes with rectangular apertures in substrates containing anisotropic materials is especially significant for temperatures near the transition temperature. Other results also have indicated that dielectric anisotropy effect is especially significant when the size of the aperture is similar to that of the

Table 3: Resonant frequencies of high T_c superconducting rectangular microstrip patch printed on anisotropic Pyrolytic boron nitride over ground planes with and without rectangular apertures; $a \times b = 1.5\,\text{cm} \times 1\,\text{cm}$, $d = 1\,\text{mm}$, $\sigma_n = 10^6\,\text{S/m}$, $\lambda_0 = 140\,\text{nm}$, $T_c = 89\,\text{K}$, $e = 350\,\text{nm}$, and $T = 50\,\text{K}$.

Aperture size $a_a \times b_a$	Resonant frequencies (GHz)		Fractional change (%)
	Considering anisotropy $(\varepsilon_x, \varepsilon_z) = (5.12, 3.4)$	Neglecting anisotropy $(\varepsilon_x, \varepsilon_z) = (3.4, 3.4)$	
0	7.399	7.531	1.78
$0.25a \times 0.25b$	7.044	7.165	1.72
$0.5a \times 0.5b$	5.935	6.052	1.97
$0.75a \times 0.75b$	4.955	5.089	2.70
$a \times b$	4.277	4.510	5.45

Table 4: Resonant frequencies of different TM modes of high T_c superconducting rectangular microstrip patch printed on anisotropic Sapphire over ground plane with rectangular aperture; $a \times b = 1.5\,\text{cm} \times 1\,\text{cm}$, $a_a \times b_a = 2.1\,\text{mm} \times 1.4\,\text{mm}$, $d = 2\,\text{mm}$, $\sigma_n = 10^6\,\text{S/m}$, $\lambda_0 = 140\,\text{nm}$, $T_c = 89\,\text{K}$, $e = 350\,\text{nm}$, and $T = 40\,\text{K}$.

Mode TM_{nm}	Resonant frequencies (GHz)		Fractional change (%)
	Considering anisotropy $(\varepsilon_x, \varepsilon_z) = (9.4, 11.6)$	Neglecting anisotropy $(\varepsilon_x, \varepsilon_z) = (11.6, 11.6)$	
TM_{10}	2.946	2.909	1.26
TM_{01}	4.032	3.967	1.61
TM_{11}	5.288	5.197	1.72
TM_{20}	5.643	5.567	1.35
TM_{02}	7.626	7.453	2.27

high T_c superconducting patch. This result agrees with that discovered theoretically for perfectly conducting rectangular microstrip patches over ground planes with rectangular apertures [2]. Concerning the influence of uniaxial anisotropy in the substrate on different TM modes of the superconducting antenna, we have found that dielectric anisotropy effect is especially significant for the mode TM_{02}.

References

[1] V. Losada, R. R. Boix, and M. Horno, "Resonant modes of circular microstrip patches over ground planes with circular apertures in multilayered substrates containing anisotropie and ferrite materials," *IEEE Transactions on Microwave Theory and Techniques*, vol. 48, no. 10, pp. 1756–1762, 2000.

[2] T. Fortaki and A. Benghalia, "Rigorous full-wave analysis of rectangular microstrip patches over ground planes with rectangular apertures in multilayered substrates that contain isotropic and uniaxial anisotropic materials," *Microwave and Optical Technology Letters*, vol. 41, no. 6, pp. 496–500, 2004.

[3] S. Liu and B. Guan, "Wideband high-temperature superconducting microstrip antenna," *Electronics Letters*, vol. 41, no. 17, pp. 947–948, 2005.

[4] N. Sekiya, A. Kubota, A. Kondo, S. Hirano, A. Saito, and S. Ohshima, "Broadband superconducting microstrip patch antenna using additional gap-coupled resonators," *Physica C*, vol. 445–448, no. 1-2, pp. 994–997, 2006.

[5] O. Barkat and A. Benghalia, "Radiation and resonant frequency of superconducting annular ring microstrip antenna on uniaxial anisotropic media," *Journal of Infrared, Millimeter, and Terahertz Waves*, vol. 30, no. 10, pp. 1053–1066, 2009.

[6] F. Benmeddour, C. Dumond, F. Benabdelaziz, and F. Bouttout, "Improving the performances of a high T_c superconducting circular microstrip antenna with multilayered configuration and anisotropic dielectrics," *Progress In Electromagnetics Research C*, vol. 18, pp. 169–183, 2011.

[7] S. Benkouda, M. Amir, T. Fortaki, and A. Benghalia, "Dual-frequency behavior of stacked high T_c superconducting microstrip patches," *Journal of Infrared, Millimeter, and Terahertz Waves*, vol. 32, no. 11, pp. 1350–1366, 2011.

[8] T. Fortaki, L. Djouane, F. Chebara, and A. Benghalia, "On the dual-frequency behavior of stacked microstrip patches," *IEEE Antennas and Wireless Propagation Letters*, vol. 7, pp. 310–313, 2008.

[9] O. Barkat and A. Benghalia, "Synthesis of superconducting circular antennas placed on circular array using a particle swarm optimisation and the fullwave method," *Progress In Electromagnetics Research B*, no. 22, pp. 103–119, 2010.

[10] Ç. S. Gürel and E. Yazgan, "Resonant frequency analysis of annular ring microstrip patch on uniaxial medium via hankel transform domain immittance approach," *Progress In Electromagnetics Research M*, vol. 11, pp. 37–52, 2010.

[11] Ç. S. Gürel and E. Yazgan, "Resonance in microstrip ring resonator with uniaxially anisotropic substrate and superstrate layers," *Journal of Electromagnetic Waves and Applications*, vol. 24, no. 8-9, pp. 1135–1144, 2010.

[12] A. Motevasselian, "Spectral domain analysis of resonant characteristics and radiation patterns of a cir-cular disc and an annular ring microstrip antenna on uniaxial substrate," *Progress In Electromagnetics Research M*, vol. 21, pp. 237–251, 2011.

[13] Y. Tighilt, F. Bouttout, and A. Khellaf, "Modeling and design of printed antennas using neural networks," *International Journal of RF and Microwave Computer-Aided Engineering*, vol. 21, no. 2, pp. 228–233, 2011.

[14] L. Djouablia, I. Messaouden, and A. Benghalia, "Uniaxial anisotropic substrate effects on the resonance of an equitriangular MI-crostrip patch antenna," *Progress in Electromagnetics Research M*, vol. 24, pp. 45–56, 2012.

[15] F. Chebbara, S. Benkouda, and T. Fortaki, "Fourier transform domain analysis of high T_c superconducting rectangular microstrip patch over ground plane with rectangular aperture," *Journal of Infrared, Millimeter, and Terahertz Waves*, vol. 31, no. 7, pp. 821–832, 2010.

[16] T. Fortaki, L. Djouane, F. Chebara, and A. Benghalia, "Radiation of a rectangular microstrip patch antenna covered with a dielectric layer," *International Journal of Electronics*, vol. 95, no. 9, pp. 989–998, 2008.

[17] T. Fortaki, D. Khedrouche, F. Bouttout, and A. Benghalia, "A numerically efficient full-wave analysis of a tunable rectangular microstrip patch," *International Journal of Electronics*, vol. 91, no. 1, pp. 57–70, 2004.

[18] M. A. Richard, K. B. Bhasin, and P. C. Claspy, "Superconducting microstrip antennas: an experimental comparison of two feeding methods," *IEEE Transactions on Antennas and Propagation*, vol. 41, no. 7, pp. 967–974, 1993.